SUPPORTING INFORMATION

Predicting Reduction Rates of Energetic Nitroaromatic Compounds Using Calculated One-Electron Reduction Potentials

*Alexandra J. Salter-Blanc[1], Eric J. Bylaska[2], Hayley J. Johnston[1], and Paul G. Tratnyek[1]**

[1] Institute of Environmental Health
Oregon Health & Science University
3181 SW Sam Jackson Park Road, Portland, OR 97239-3098

[2] William R. Wiley Environmental Molecular Sciences Laboratory
Pacific Northwest National Laboratory
P.O. Box 999, Richland, WA 99352

*Corresponding author:
Email: tratnyek@ohsu.edu, Phone: 503-346-3431, Fax: 503-346-3427

Contents

02/11/2015

1. Computational Methods

The first step used to calculate the solution phase one-electron reduction potential was to calculate the free energy difference, ΔG_{rxn}, for the one-electron half reaction,

$$Ar\text{-}NO_{2(aq)} + 1e^-_{(g)} \rightarrow Ar\text{-}NO^{\bullet -}_{2(aq)}$$

directly from gas phase reaction energy, entropy, and solvation energy differences using electronic structure calculations, gas phase entropy estimates, and continuum solvation models. The NWChem program suite was used for all of these calculations.[1] The electronic structure calculations were carried out using density functional theory (DFT) calculations[2] with the 6-311++G(2d,2p) basis set[3, 4] and the LDA,[5] PBE96,[6] B3LYP,[7, 8] PBE0,[9] and M06-2X[10] exchange correlation functionals. The choice of basis set is somewhat larger than typically used for these types of calculations; however, modest size parallel computers can easily augment the extra computational expense incurred for the size of molecules considered in this study. The choice of exchange correlation potentials covers a wide range of exchange-correlation types popular in the literature. Two classes of potentials not explored in this study—that have recently received attention—include the range corrected exchange correlation potentials and the related approach where the exact exchange term is adjusted to produce the correct derivative discontinuity for the system. While these potentials have had some notable successes and their development is on-going, how and where to best use them is still not clear (e.g. range corrected exchange correlation potentials dramatically fail in the condensed phase).

Solvation energies for solutes that do not react strongly with water can be approximated as a sum of non-covalent electrostatic, cavitation, and dispersion energies. The electrostatic contributions to the solvation energies were estimated by using the self-consistent reaction field theory of Klamt and Schüürmann (COSMO),[11] with the cavity defined by a set of overlapping atomic spheres with radii suggested by Stefanovich and Truong[12] (H 1.172Å, C- 2.096Å, C= 1.635Å, O 1.576 Å, and Cl 1.750Å). The dielectric constant of water used for all of the solvation calculations was 78.4.[11] The cavitation and dispersion contributions to the solvation energy are less straightforward to handle because the interactions take place at short distances, and several methods have been proposed to do this.[13-20] One of the simplest approaches for estimating these terms is to use empirically derived expressions that depend only the solvent accessible surface area. In this study, the widely used formula of Sitkoff *et al.*[18] was used,

$$\Delta G_{cav+disp} = \gamma A + b$$

where *g* and *b* are constants set to 5 cal/mol-Å^2 and 0.86 kcal/mol respectively. Sitkoff *et al.* parameterized the constants *g* and *b* to the experimentally determined free energies of solvation of alkanes[21] by using a least-squares fit. The Shrake-Rupley algorithm was used to determine the solvent accessible surface areas.[22] In addition to this approach for solvation, we also calculated the one electron potentials using the COSMO-SMD approach of Marenich et. al.[23] (for the B3LYP and M06-2X exchange correlation potentials).

The reaction energy was then converted to a redox potential using

$$E_{(abs)} = -\frac{\Delta G_{rxn}}{nF}$$

where *n* is the number of electrons transferred and *F* is the Faraday constant. This type of potential is known in electrochemistry as an absolute potential ($E_{(abs)}$) and is difficult to measure directly. Instead redox potentials are usually measured relative to a reference electrode, such as the standard hydrogen electrode (SHE), saturated calomel electrode (SCE), or silver/silver-chloride electrode. For measurements using the SHE this means that the free energy differences for the one-electron half reaction are reported in terms of the following overall reaction,

$$Ar\text{-NO}_{2(\text{aq})} + \frac{1}{2}H_{2(g)} \rightarrow Ar\text{-NO}^{\bullet-}_{2(\text{aq})} + H^{+}_{(aq)}$$

the SHE potential is given by

$$E_{SHE} = E_{(abs)} + E_H^0$$

where E_H^0 is the potential associated with the absolute free energy of the hydrogen electrode reaction.

$$\tfrac{1}{2}\text{H}_{2(\text{g})} \xrightarrow{\Delta G_{rxn}} \text{H}^{+}_{(\text{aq})} + e^{-}_{(g)} \qquad E_H^0 = -\frac{\Delta G_{rxn}}{F}$$

The exact value for E_H^o remains unknown despite extensive experimental and computational efforts. In this study, a value of $E_H^0 = 98.6$ kcal/mol was used. This value was estimated using

value of $\Delta G_s\left(\mathrm{H}^+\right) = -263.98$ kcal/mol reported by Tissandier et al.,[24] along with the gas phase values of $\Delta_f G^0\left(\mathrm{H}^+_{(g)}\right)$ and $\Delta_f G^0\left(\mathrm{H}_{2(g)}\right)$, i.e.,

$$\begin{aligned} E_H^0 &= \Delta G_s\left(\mathrm{H}^+\right) + \left(\Delta_f G^o\left(\mathrm{H}^+_{(g)}\right) - \Delta_f G^o\left(\mathrm{H}_{2(g)}\right)\right) \\ &= -263.98 \text{ kcal/mol} + 362.58 \text{ kcal/mol} \\ &= 98.6 \text{ kcal/mol} \end{aligned}$$

2. Data and Calculation Details for Figure 2

Table S1. Data and calculation details for juglone.

NAC	E^1_{NAC} [a]	$\Delta G^{\circ\prime}$ [b]	k_{JUG} (M^{-1} s^{-1})	log(k_{JUG})	Experimental pH [c]
NB	−0.485 [d]	9.04	0.079	−1.1	6.79 ± 0.02
2-CH_3-NB	−0.590 [d]	11.5	0.003	−2.5	6.79 ± 0.02
3-CH_3-NB	−0.475 [d]	8.81	0.12	−0.92	6.79 ± 0.02
4-CH_3-NB	−0.500 [d]	9.39	0.051	−1.3	6.79 ± 0.02
2-Cl-NB	*−0.485* [d]	9.04	0.15	−0.82	6.79 ± 0.02
3-Cl-NB	−0.405 [d]	7.20	1.3	0.11	6.79 ± 0.02
4-Cl-NB	−0.450 [d]	8.23	0.5	−0.30	6.79 ± 0.02
2-$COCH_3$-NB	*−0.470* [d]	8.69	0.35	−0.46	6.79 ± 0.02
3-$COCH_3$-NB	*−0.405* [d]	7.20	2.5	0.38	6.79 ± 0.02
4-$COCH_3$-NB	−0.360 [d]	6.16	30	1.5	6.79 ± 0.02
TNT	*−0.300* [e]	4.77	740	2.9	6.60
2-ADNT	*−0.390* [e]	6.85	9.7	0.99	6.60
4-ADNT	*−0.430* [e]	7.77	1.2	0.079	6.60
2,4-DANT	*−0.515* [e]	9.73	0.021	−1.7	6.60
2,6-DANT	*−0.495* [e]	9.27	0.056	−1.3	6.60
4-CH_3-NB	−0.500 [e]	9.39	0.047	−1.3	6.60
4-Cl-NB	−0.450 [e]	8.23	0.48	−0.32	6.60
4-$COCH_3$-NB	−0.358 [e]	6.11	51	1.7	6.60
1,3-DNB	−0.345 [e]	5.81	61	1.8	6.60
1,4-DNB	−0.257 [e]	3.78	6900	3.8	6.60
2-NH_2-NB	*(<−0.560)* [e]		0.0023	−2.6	6.60
3-NH_2-NB	*−0.500* [e]	9.39	0.043	−1.4	6.60

a) Estimated E^1_{NAC} in italics.

b) Calculated using $E^1_{red} = E^1_7 = -0.093$ V.[25] A similar value (−0.095 V) has also been reported.[26]

c) Used in determining k_{JUG}.

d) From Schwarzenbach et al. (1990)[27] and references cited therein.

e) From Hofstetter et al. (1999)[28] and references cited therein.

Table S2. Data and calculation details for lawsone.

NAC	E^1_{NAC} [a]	$\Delta G^{\circ\prime}$ [b]	k_{LAW} (M^{-1} s^{-1})	log(k_{LAW})	Experimental pH [c]
NB	−0.485	1.61	2.4	0.38	6.98 ± 0.02
2-CH_3-NB	−0.590	4.04	0.037	−1.4	6.98 ± 0.02
3-CH_3-NB	−0.475	1.38	2.9	0.46	6.98 ± 0.02
4-CH_3-NB	−0.500	1.96	1.1	0.041	6.98 ± 0.02
2-Cl-NB	*−0.485*	1.61	2.2	0.34	6.98 ± 0.02
3-Cl-NB	−0.405	−0.231	31	1.5	6.98 ± 0.02
4-Cl-NB	−0.450	0.807	11	1.0	6.98 ± 0.02
2-$COCH_3$-NB	*−0.470*	1.27	3.3	0.52	6.98 ± 0.02
3-$COCH_3$-NB	*−0.405*	−0.231	46	1.7	6.98 ± 0.02
4-$COCH_3$-NB	−0.360	−1.27	330	2.5	6.98 ± 0.02

a) From Schwarzenbach et al. (1990)[27] and references cited therein. Estimated E^1_{NAC} in italics.

b) Calculated using $E^1_{red} = E^1_7 = -0.415$ V.[26]

c) Used in determining k_{LAW}

Table S3. Data and calculation details for AQDS.

NAC	E^1_{NAC} [a]	$\Delta G^{\circ\prime}$ [b]	k_{LAW} (M^{-1} s^{-1})	log(k_{LAW})	Experimental pH [c]
2-CH3-NB	-0.590 [d]	7.794	5.95	0.774517	5
4-CH3-NB	-0.500 [d]	5.719	66.3	1.82151	5
2-Cl-NB	*-0.485* [d]	5.373	258	2.41162	5
4-Cl-NB	-0.450 [d]	4.566	972	2.98767	5
1,2-DNB			255000	5.40654	5
TNT	*-0.300* [e]	1.107	160000	5.20412	5

a) Estimated E^1_{NAC} in italics.

b) Calculated using $E^1_{red} = -0.252$ V, which was determined for pH 5 using a modeled standard one-electron potential (E^1_0) of −0.13359 V for $AHQDS^{\bullet} + e^- \leftrightarrow AHQDS^-$ [29] and the following equation:

$$E^1_{red} = E^1_0 + \frac{RT}{nF}\log\frac{[AHQDS^{\bullet}][H^+]}{[AH_2QDS]}$$

c) Used in determining k_{AQDS}

d) From Schwarzenbach et al. (1990)[27] and references cited therein. Estimated E^1_{NAC} in italics.

e) From Hofstetter et al. (1999)[28] (estimated E^1_{NAC}).

Table S4. Data and calculation details for iron porphyrin.

NAC	E^1_{NAC} [a]	$\Delta G^{\circ\prime}$ [b]	$k_{Fe(II)P}$ (M^{-1} s^{-1})	log($k_{Fe(II)P}$)	Experimental pH [c]
NB	−0.485	12.7	0.96	−0.018	7.01 ± 0.02
2-CH_3-NB	−0.590	15.1	0.25	−0.60	7.01 ± 0.02
3-CH_3-NB	−0.475	12.5	1.1	0.041	7.01 ± 0.02
4-CH_3-NB	−0.500	13.0	0.67	−0.17	7.01 ± 0.02
2-Cl-NB	*−0.485*	12.6	8.8	0.94	7.01 ± 0.02
3-Cl-NB	−0.405	10.8	5.3	0.72	7.01 ± 0.02
4-Cl-NB	−0.450	11.9	2.7	0.43	7.01 ± 0.02
2-$COCH_3$-NB	*−0.470*	12.3	23.8	1.38	7.01 ± 0.02
3-$COCH_3$-NB	*−0.405*	10.8	6.3	0.80	7.01 ± 0.02
4-$COCH_3$-NB	−0.360	9.80	19.3	1.29	7.01 ± 0.02

a) From Schwarzenbach et al. (1990)[27] and references cited therein. Estimated E^1_{NAC} in italics.

b) Calculated using $E^1_{red} = E^{1\prime}$ (one-electron reduction potential under standard environmental conditions) = 0.065 V.[27]

c) Used in determining $k_{Fe(II)P}$.

Table S5. Data and calculation details for Fe(II)/tiron.

NAC	E^1_{NAC} [a]	$\Delta G^{\circ\prime}$ [b]	log(k_{tiron}) (k in M^{-1} s^{-1})	Experimental pH [c]
4-Cl-NB	−0.450	−5.24	4.4	5.76
4-$COCH_3$-NB	−0.360	−7.31	6.3	5.76
3-Cl-NB	−0.405	−6.27	4.9	5.76
3-CH_3-NB	−0.475	−4.66	3.8	5.76
NB	−0.485	−4.43	4.0	5.76
4-CH_3-NB	−0.500	−4.08	3.5	5.76

a) Measured at pH 7. Correction to pH 5.76 according to methods previously reported[30] did not significantly change the value.

b) Calculated using E^1_{red} of −0.677 V, which was determined from the following equation[31]:

$$E^1_{red} = +0.77 - \frac{RT}{F}\ln\left(\frac{\{Fe^{2+}\}}{\{Fe^{3+}\}}\right)$$

where E^1_{red} is the non-standard, "condition-dependent" reduction potential and +0.77 is the standard one-electron reduction potential for Fe(III)/Fe(II). $\{Fe^{2+}\}$ and $\{Fe^{3+}\}$ were determined through speciation modeling performed in Geochemist's Workbench (release 8.0) with the thermo.com.v8.r6+ thermodynamic dataset with added stability constants for tiron from Naka et al., 2006.[32] Our speciation model appeared to deviate from that used by Naka et al. (based on comparison to Figure 3D from Naka et al. (2009)). Comparing our Geochemist's Workbench model with a model produced using MINEQL+ (which agreed with Figure 3D from Naka et al. (2009)) it appears the models use different stability constants for the solid phases in the system.

c) Used in determining k_{tiron}.

Table S6. Data and calculation details for Fe(II)/DFOB.

NAC	E^1_{NAC} [a]	$\Delta G^{\circ\prime}$ [b]	$\log(k_{DFOB})$ (k in $M^{-1} s^{-1}$)	Experimental pH [c]
3-Cl-NB	−0.405	−1.43	2.9	9.03
4-Cl-NB	−0.450	−0.392	2.5	9.03
NB	−0.485	0.415	2.2	9.03
3-CH_3-NB	−0.475	0.184	2.1	9.03
4-CH_3-NB	−0.500	1.07	2.0	9.03

a) Measured at pH 7. Correction to pH 9.03 according to methods previously reported [30] did not significantly change the value.

b) Calculated using E^1_{red} of −0.480 V, which was determined using the equation discussed in the footnotes to Table S5. Additional stability constants for DFOB were obtained from Kim et al. (2009).[33] Our speciation model (modeled with Geochemist's Workbench) appeared to accurately reproduce Figure 3B from Kim et al. (2009) suggesting agreement of our model to the model used by Kim et al.

c) Used in determining k_{DFOB}.

3. Comparison of Calculated and Measured E^1_{NAC}

Table S7. Determination of largest positive and negative error in Table 1. Largest positive errors are shown in bold and denoted with a dagger (†); largest negative errors are shown in bold and denoted with a double dagger (‡).

	Error (Calculated E^1_{NAC} − Measured E^1_{NAC}) (V)						
	LDA	**PBE**	**B3LYP**	**PBE0**	**M06-2X**	**B3LYP**	**M06-2X**
Abbr.			COSMO			COSMO-SMD	
NB	-0.026	-0.154	0.007	-0.092	0.010	0.084	0.082
2-CH_3-NB	-0.069	-0.181	-0.026	-0.105	-0.040	0.042	-0.029
3-CH_3-NB	-0.086	-0.215	-0.047	-0.127	-0.015	0.031	0.037
4-CH_3-NB	-0.094	-0.226	-0.069	-0.137	-0.052	0.031	0.035
3-Cl-NB	0.133	-0.140	0.005	-0.082	-0.166	0.064	0.055
4-Cl-NB	-0.025	-0.149	0.006	-0.089	0.010	0.068	0.062
4-NH_2-NB	**-0.396** ‡	-0.475	-0.185	-0.295	-0.169	-0.101	**-0.208** ‡
3-$COCH_3$-NB	-0.002	-0.149	-0.032	-0.101	-0.023	0.052	0.061
4-$COCH_3$-NB	0.182	0.002	0.052	-0.019	0.004	0.134	0.095
1,2-DNB	0.320	0.118	0.166	0.057	-0.012	0.271	0.130
1,3-DNB	0.006	-0.236	-0.045	-0.160	-0.039	0.180	0.102
1,4-DNB	**0.454** †	**0.268** †	**0.316** †	**0.182** †	**0.140** †	**0.388** †	**0.205** †
2,4-DNT	-0.145	-0.241	-0.089	-0.221	-0.007	-0.044	0.080
2,6-DNT	0.084	-0.316	-0.167	-0.280	-0.123	-0.111	-0.005
TNT	0.021	-0.131	0.030	-0.125	0.001	0.062	0.100
2-CHO	0.204	0.010	0.084	-0.006	0.014	0.130	0.083
4-CHO	0.257	0.067	0.106	0.049	-0.042	0.196	0.093
4-CH_2OH	-0.076	-0.164	-0.023	-0.146	-0.083	0.059	0.020
2-ADNT	-0.169	-0.312	-0.137	-0.225	-0.049	-0.063	0.033
4-ADNT	-0.258	-0.304	-0.180	-0.251	-0.122	-0.074	-0.018
2,4-DANT	-0.368	**-0.493** ‡	**-0.308** ‡	**-0.374** ‡	**-0.273** ‡	**-0.195** ‡	0.037

4. NAC Disappearance Data

Table S8. Concentration vs. time data for the disappearance of NACs at different [FeP] and the associated k_{obs} vs. [FeP] plots used to determine $k_{Fe(II)P}$. In cases where only the initial portion of the concentration vs. time data was fit to the pseudo-first-order model (denoted with asterisks) a "zoomed-in" plot of the fitted data is also shown.

NAC	Conc. vs. time plot	k_{obs} vs. [FeP] plot
NB	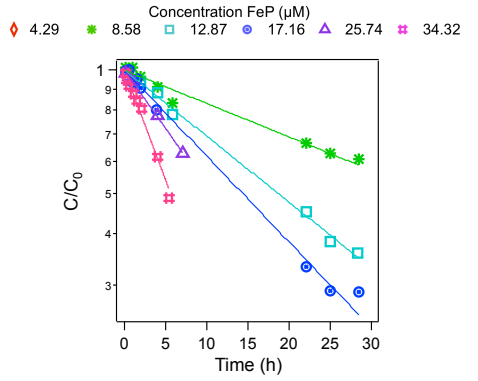	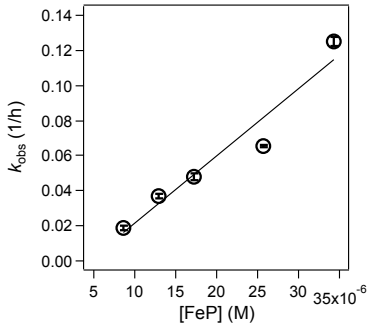
4-Cl-NB	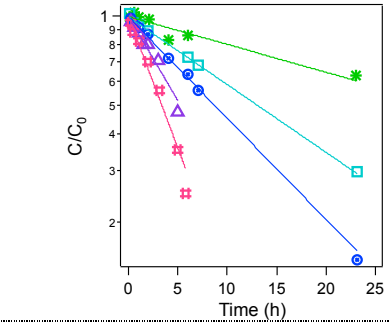	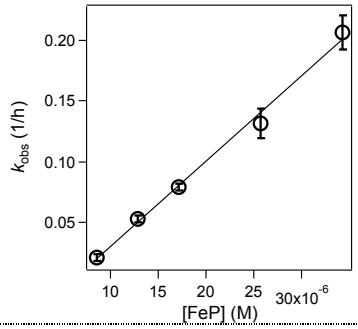
1,3-DNB*	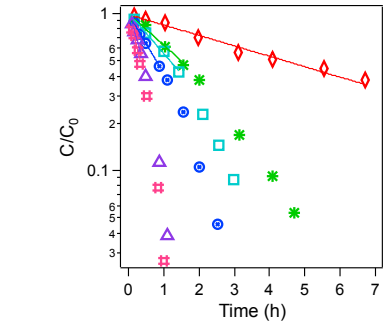 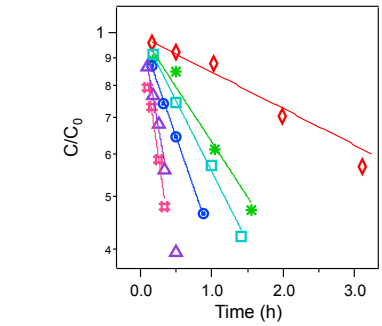	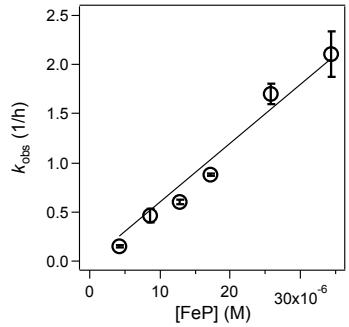

2,4-DNT

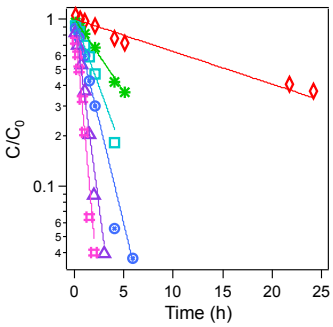

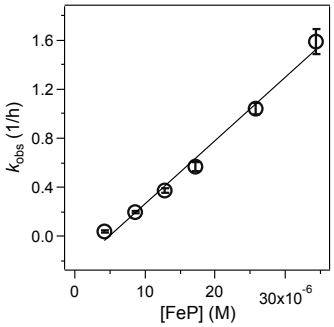

TNT*

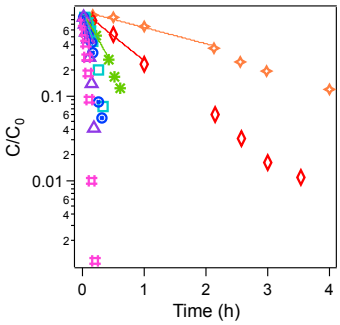

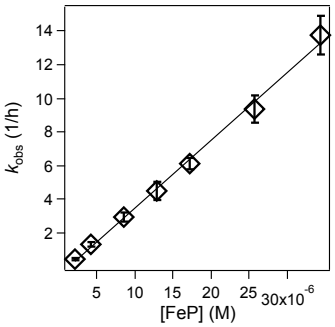

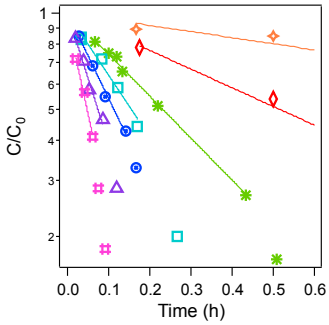

DNAN*

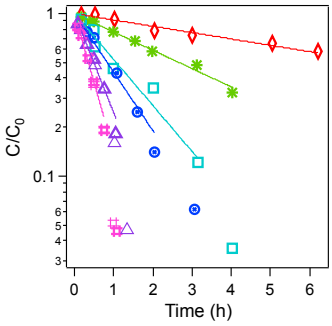

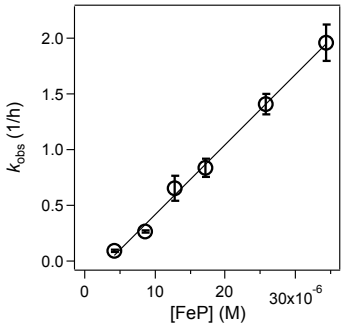

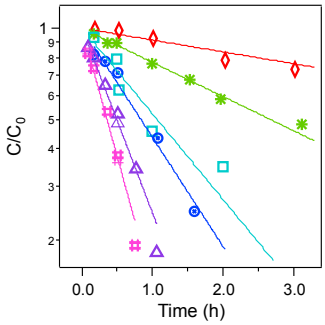

References in the Supporting Information

(1) Valiev, M.; Bylaska, E. J.; Govind, N.; Kowalski, K.; Straatsma, T. P.; Van, D. H. J. J.; Wang, D.; Nieplocha, J.; Apra, E.; Windus, T. L.; de Jong, W. A. NWChem: A comprehensive and scalable open-source solution for large scale molecular simulations. *Comput. Phys. Commun.* **2010**, *181*, 1477-1489.

(2) Kohn, W.; Sham, L. J. Self-consistent equations including exchange and correlation effects. *Phys. Rev. B* **1965**, *A140*, 1133-1138.

(3) Clark, T.; Chandrasekhar, J.; Spitznagel, G. W.; Schleyer, P. v. R. Efficient diffuse function-augmented basis sets for anion calculations. III. The 3-21 + G basis set for first-row elements, lithium to fluorine. *J. Comput. Chem.* **1983**, *4*, 294-301.

(4) Krishnan, R.; Binkley, J. S.; Seeger, R.; Pople, J. A. Self-consistent molecular orbital methods. XX. A basis set for correlated wave functions. *J. Chem. Phys.* **1980**, *72*, 650.

(5) Vosko, S. H.; Wilk, L.; Nusair, M. Accurate spin-dependent electron liquid correlation energies for local spin density calculations: a critical analysis. *Can. J. Phys.* **1980**, *58*, 1200-1211.

(6) Perdew, J. P.; Burke, K.; Ernzerhof, M. Generalized gradient approximation made simple. *Phys. Rev. Lett.* **1996**, *77*, 3865.

(7) Becke, A. D. Density-functional thermochemistry 3. The role of exact exchange. *J. Chem. Phys.* **1993**, *98*, 5648-5652.

(8) Lee, C.; Yang, W.; Parr, R. G. Development of the Colle-Salvetti correlation-energy formula into a functional of electron density. *Phys. Rev. B* **1988**, *37*, 785-789.

(9) Adamo, C.; Barone, V. Toward reliable density functional methods without adjustable parameters: The PBE0 model. *The Journal of Chemical Physics* **1999**, *110*, 6158.

(10) Zhao, Y.; Truhlar, D. G. The M06 suite of density functionals for main group thermochemistry, thermochemical kinetics, noncovalent interactions, excited states, and transition elements: two new functionals and systematic testing of four M06-class functionals and 12 other functionals. *Theor. Chem. Acc.* **2008**, *120*, 215-241.

(11) Klamt, A.; Schüürmann, G. COSMO: A new approach to dielectric screening in solvents with explicit expressions for the screening energy and its gradient. *J. Chem. Soc., Perkin Trans. 2* **1993**, 799-803.

(12) Stefanovich, E. V.; Truong, T. N. Optimized atomic radii for quantum dielectric continuum solvation models. *Chem. Phys. Lett.* **1995**, *244*, 65-74.

(13) Pierotti, R. A. Aqueous solutions of nonpolar gases. *J. Phys. Chem.* **1965**, *69*, 281-288.

(14) Huron, M. J.; Claverie, P. Calculation of the interaction energy of one molecule with its whole surrounding. II. Method of calculating electrostatic energy. *J. Phys. Chem.* **1974**, *78*, 1853-1861.

(15) Floris, F. M.; Tomasi, J.; Pascual Ahuir, J. L. Dispersion and repulsion contributions to the solvation energy: Refinements to a simple computational model in the continuum approximation. *J. Comput. Chem.* **1991**, *12*, 784-791.

(16) Honig, B.; Sharp, K. A.; Yang, A. Macroscopic models of aqueous solutions: Biological and chemical applications. *J. Phys. Chem.* **1993**, *97*, 1101-1109.

(17) Tomasi, J.; Persico, M. Molecular interactions in solution: An overview of methods based on continuous distributions of the solvent. *Chem. Rev.* **1994**, *94*, 2027-2094.

(18) Sitkoff, D.; Sharp, K. A.; Honig, B. Accurate calculation of hydration free energies using macroscopic solvent models. *J. Phys. Chem.* **1994**, *98*, 1978-1988.

(19) Cramer, C. J.; Truhlar, D. G. Implicit solvation models: Equilibrium, structure, spectra, and dynamics. *Chem. Rev.* **1999**, *99*, 2161-2200.

(20) Eckert, F.; Klamt, A. Fast solvent screening via quantum chemistry: COSMO-RS approach. *AIChE J.* **2002**, *48*, 369-385.

(21) Ben-Naim, A.; Marcus, Y. Solvation thermodynamics of nonionic solutes. *J. Chem. Phys.* **1984**, *81*, 2016-2027.

(22) Shrake, A.; Rupley, J. A. Environment and exposure to solvent of protein atoms. Lysozyme and insulin. *J. Mol. Biol.* **1973**, *79*, 351-364.

(23) Marenich, A. V.; Cramer, C. J.; Truhlar, D. G. Universal solvation model based on solute electron density and on a continuum model of the solvent defined by the bulk dielectric constant and atomic surface tensions. *J. Phys. Chem. B.* **2009**, *113*, 6378-6396.

(24) Tissandier, M. D.; Cowen, K. A.; Feng, W. Y.; Gundlach, E.; Cohen, M. H.; Earhart, A. D.; Coe, J. V.; Tuttle, T. R. The proton's absolute aqueous enthalpy and Gibbs free energy of solvation from cluster-ion solvation data. *J. Phys. Chem. A* **1998**, *102*, 7787-7794.

(25) Mukherjee, T. One-electron reduction of juglone (5-hydroxy-1,4-naphthoquinone): A pulse radiolysis study. *Radiat. Phys. Chem.* **1987**, *29*, 455-462.

(26) Ölinger, K.; Buffington, G. D.; Ernster, L.; Cadenas, E. Effects of superoxide dismutase on the automation of substituted hydro- and semi-naphthoquinones. *Chem.-Biol. Interact.* **1990**, *73*, 53-76.

(27) Schwarzenbach, R. P.; Stierli, R.; Lanz, K.; Zeyer, J. Quinone and iron porphyrin mediated reduction of nitroaromatic compounds in homogeneous aqueous solution. *Environ. Sci. Technol.* **1990**, *24*, 1566-1574.

(28) Hofstetter, T. B.; Heijman, C. G.; Haderlein, S. B.; Holliger, C.; Schwarzenbach, R. P. Complete reduction of TNT and other (poly)nitroaromatic compounds under iron-reducing subsurface conditions. *Environ. Sci. Technol.* **1999**, *33*, 1479-1487.

(29) Batchelor-McAuley, C.; Li, Q.; Dapin, S. M.; Compton, R. G. Volummetric characterization of DNA intercalators across the full pH range: Anthraquinone-2,6-disulfonate and anthraquinone-2-sulfonate. *J. Phys. Chem. B.* **2010**, *114*, 4094.

(30) Meisel, D.; Neta, P. One-electron redox potentials of nitro compounds and radiosensitizers. Correlation with spin densities of their radical anions. *J. Am. Chem. Soc.* **1975**, *97*, 5198-5203.

(31) Strathmann, T. J. Redox reactivity of organically complexed iron(II) species with aquatic contaminants. In: *Aquatic Redox Chemistry*; Tratnyek, P. G.; Grundl, T. J.; Haderlein, S. B., Eds.; American Chemical Society: Washington, DC, **2011**; ACS Symposium Series,

Vol. 1071; pp. 283-313.

(32) Naka, D.; Kim, D.; Strathmann, T. J. Abiotic reduction of nitroaromatic compounds by aqueous iron(ll)-catechol complexes. *Environ. Sci. Technol.* **2006**, *40*, 3006-3012.

(33) Kim, D.; Duckworth, O. W.; Strathmann, T. J. Hydroxamate siderophore-promoted reactions between iron(II) and nitroaromatic groundwater contaminants. *Geochim. Cosmochim. Acta* **2009**, *73*, 1297-1311.